J. KAU: Mar. Sci., **vol. 13,** pp. 93-110 (1422 A.H. / 2002 A.D.)

Mineralogical Investigation and Some Sedimentary Phenomena of Ubhur Formation, North Jeddah, Saudi Arabia

R.J. TAJ*, M.A . EL ASKARY**
N.A. SAAD** and M.H. BASYONI*
**Faculty of Earth Sciences, King Abdulaziz University, Jeddah, Saudi Arabia*
***Geology Department, Faculty of Science, Alexandria University, Alex., Egypt*

ABSTRACT. Clay and evaporite components of Ubhur Formation are investigated. Their mineralogy is studied by X-ray diffraction, differential thermal and thermogravimetric analyses. The clay deposits are found to be made up mainly of montmorillonite (Ca^{++} and / or Mg^{++} rich variety) with lesser amounts of illite and kaolinite while chlorite is rarely recorded in minor amounts. Spheroidal weathering believed to be formed as a result of expansion of montmorillonite by simply absorbing water, combined with leaching of some coarse ingredients and some mineralogical changes, characterizes the clay outcrops. Evaporite deposits are represented by two gypsum varieties; one comprising massive, finely crystalline gypsum, the other pure selenite. The uppermost exposed selenite shows diagenetically-formed desert roses. It is suggested that they were formed as a result of dissolution of calcium sulphate in percolating groundwater, which was drawn to the surface and precipitated gypsum during very dry spells. Results of thermogravimetric analysis of different prepared selenite concentrations gave a perfect linear relation between concentration and TG loss percent, which can be used to estimate precisely the gypsum content in any unknown sample.

Introduction

The present paper is extracted from the final report of KAAU-sponsored research project No. 203/419 submitted by the same authors (Taj *et al*., 2001a) which concerned with the sedimentology, mineralogy, chemistry and industrial

applications of the Tertiary clay deposits in Makkah and Rabigh quadrangles. The economic potentiality of these clay deposits is published by Taj *et al*. (2001b).

Among the sedimentary rocks forming the Ubhur Formation, clay and evaporite deposits represent two major components. The mineralogy and the sedimentary phenomena characterizing these deposits are the subject of the present investigation. The mineralogy of the clay deposits of the other Tertiary formations (Haddat Ash Sham, Usfan, Shumaysi, Khulays, Buraykah and Daffin) is published by Basyoni *et al*. (2002). Based on the content of several trace elements and geochemical relations between some of them, especially boron, gallium and rubidium, Ubhur Formation is supposed to be deposited under transitional to marine environments (Taj *et al*., 2002).

Geology and Sampling

The Ubhur Formation is one of the Tertiary formations lying in Makkah quadrangle, which is located in the west-central part of the Arabian Shield bordering the Red Sea (Fig. 1). The quadrangle comprises Precambrian basement rocks unconformably overlain by Tertiary sedimentary rocks which are exposed sporadically, and usually poorly, beneath a cover of flat-lying lavas and Quaternary deposits in the west (Moore and Al-Rehaili, 1989).

The Ubhur Formation as quoted from Moore and Al-Rehaili (1989) is poorly exposed in the northwest corner of Makkah quadrangle where it is covered with Al Harrat lava flow. Outcrops are only seen at quarries, which show that Ubhur Formation consists of green sandy clay, siltstone and soft, white bioclastic limestone with gypsum bed interbedded with the clay. Based on the microfossils and bivalves present in the limestone, Andreieff (1983) assigned an Early Miocene age to the Ubhur Formation. Spencer and Vincent (1984) believe that the exposed part of the Ubhur Formation at Al Harrat represents a small part of thick evaporitic sequence, attaining 77 meters thickness, deposited in Tihama beneath the coastal plain north and south of Jeddah.

Four localities (UB1, UB2, UB3, & UB4, Fig. 1) from Ubhur Formation are sampled and investigated. Some sedimentary phenomena are recorded and described.

The First Locality UB1

The succession at UB1 is made up mainly of slightly fissile silty or sandy clay with different colours; brown, yellow, white and locally purple with carbonate nodules. It is capped with basalt blocks of the Harrat Al-Harrat (Plate 1a).

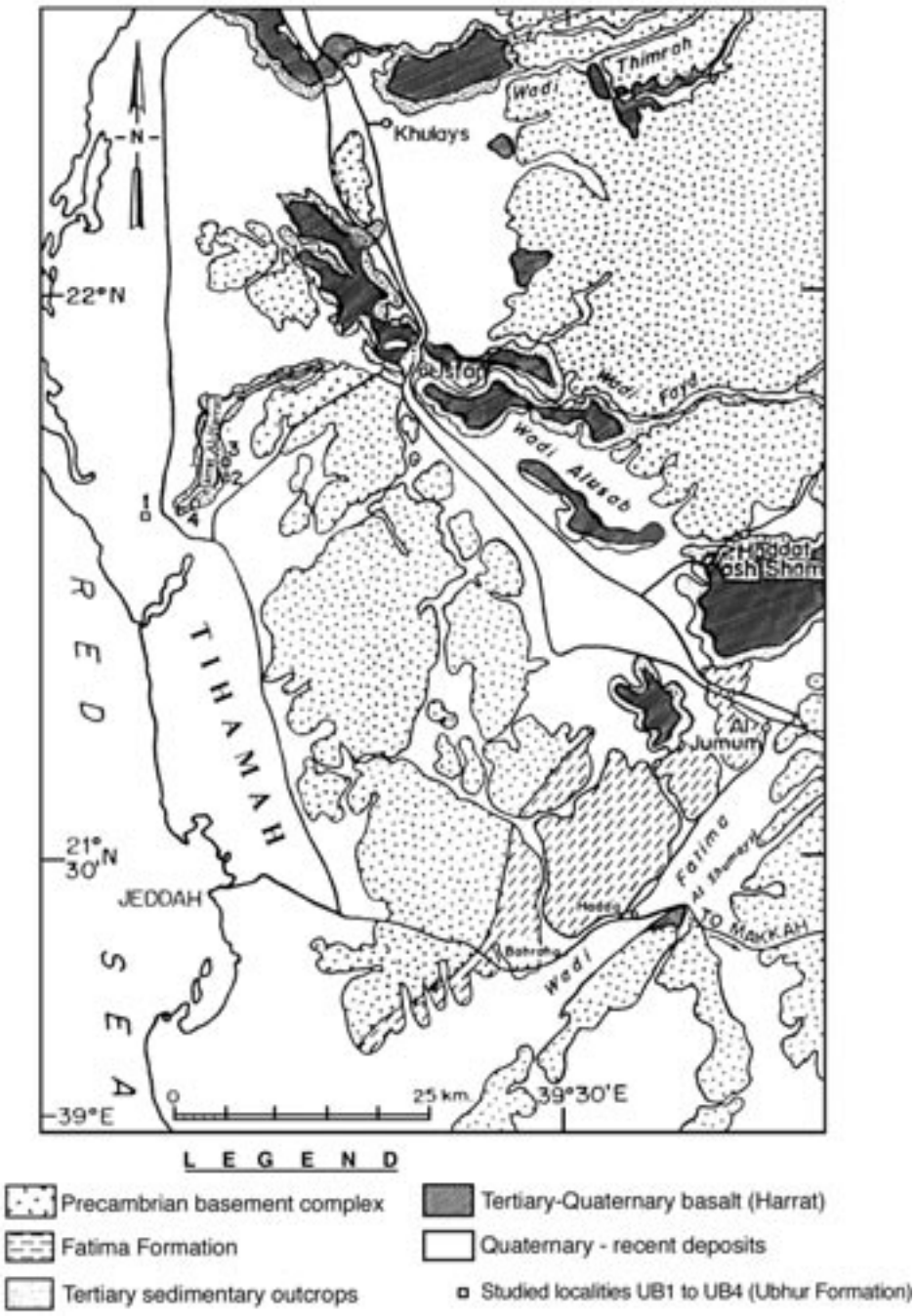

FIG. 1. Simplified geological map showing the location of the studied localities (UB1 to UB4) of Ubhur Formation (after Brown *et al.,* 1963, with modification).

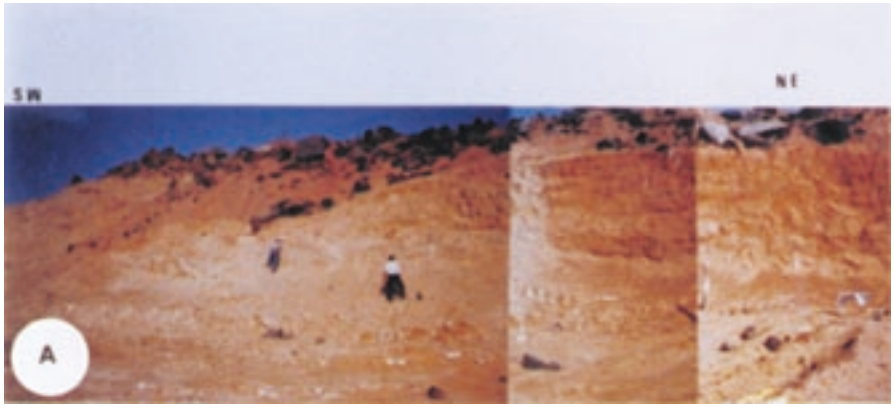

Plate 1a. Panorama of the exposed Ubhur Formation, extends from SW to NE formed mainly of slightly fissile silty and sandy clay with different colors; brown, yellow and white. Basalt blocks of the Harrat Al-Harrat cap the succession, locality UB1.

Numerous gypsum and carbonate filled fractures arranged in a more or less parallel orientation cut the rocks of the succession. Several small siliceous nodules are also present in the succession (Plate 1b). Gypsum filling fractures in argillaceous rocks can be formed by the action of acidic groundwater, reacting with calcium either from the carbonate nodules within the argillaceous rocks or from intercalated limy beds.

Plate 1b. Slightly fissile, brown to brownish white, silty to sandy clay of Ubhur Formation dissected by oriented fractures filled with carbonate and gypsum. Siliceous small nodules are also interbedded, locality UB1.

The Second Locality UB2

Outcrops of massive gypsum and selenite are present at this locality beneath Harrat Al- Harrat, and it is possible that the Ubhur Formation of UB2 represents a small exposed part of a thick evaporitic sequence. The gypsum is closely asso-

ciated with clay and fine-grained sandstone. Plate 1c shows the old gypsum quarry exposure of the United Arabian Cement Plant Limited, in Ubhur Formation, which consists mainly of two varieties of gypsum with olive-grey clay and medium-grained calcareous sandstone intercalations. This quarry section revealed the following succession: green clay of uncertain thickness forming the floor, overlain by 3 meters of massive dark grey, finely crystalline gypsum, overlain by four meters of finely bedded alternating clay and undulated to enterolithic selenitic gypsum bands up to 50 cm thick, followed by sand and reddish sandy clay, covered with basalt boulders. Shearman (1980) showed that the enterolithic structures are common in secondary gypsum rocks seen at outcrops, *i.e*., in gypsum rocks that resulted from late, near surface hydration of former anhydrite rocks.

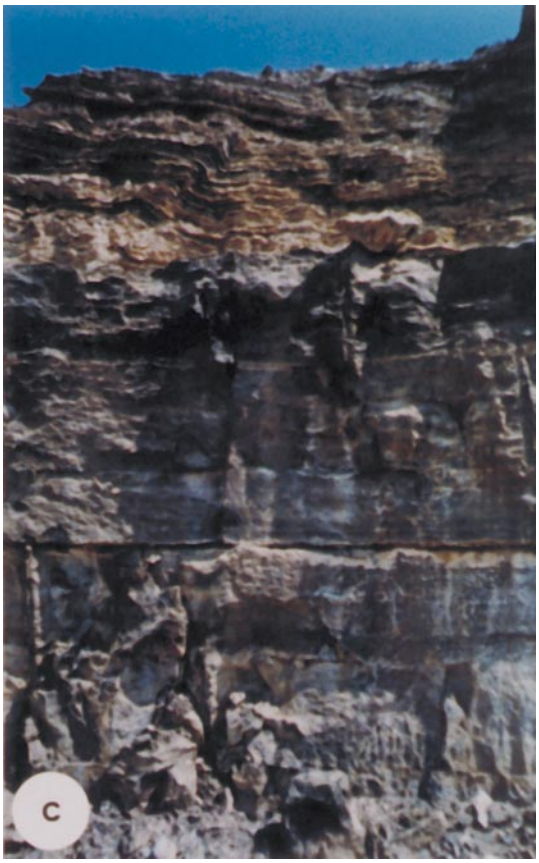

Plate 1c. The old gypsum quarry exposure of the United Arabian Cement Plant Limited (locality UB2) showing an olive grey clay bed at the base, overlain by two gypsum varieties with a separating calcareous sandstone band. The lower gypsum variety is of fine grained nature, while it is selenitic and showing undulated bedding and enterolithic folding near the top. A thin greenish clay band separates the two gypsum varieties.

A channel sample from the massive (3 m) gypsum visible in the working face of the quarry is shown by Spencer and Vincent (1984) to contain 95% gypsum, which falls within industrial plaster specifications. The four meters of alternating clay and selenitic gypsum shows over 18% impurities and is clearly less suitable, but sufficiently pure for use in cement industry. We add that the highly crystalline selenitic gypsum can be easily separated from the alternating silty clay, and in this case it will meet several industrial specifications.

The topmost exposed part of the selenite bands shows a diagenetically-formed structure of radially symmetric group of crystals (slits) with a fancied resemblance to a rose. It is believed that such structures, refered to as "desert roses" are formed when calcium sulphate dissolved in percolating groundwater is drawn to the surface and deposit as gypsum (Plate 1d) during very dry spells. Rouchy (1980) recorded similar selenitic banks showing internal crystalline arrangement in fans in the evaporitic sequences of the terminal Miocene of Sicily and of Southern Spain.

Plate 1d. Desert roses, radially symmetric group of gypsum crystals (slits) are drawn to the surface of the succession and deposited during the dry spells, locality UB2..

The Third and Fourth Localities UB3 & UB4

The rock exposures at these two localities overlie the evaporitic succession of UB2. These exposures are formed of silty to sandy clay beds showing fairly common spheroidal weathering (Plate 1e) only on the outermost, freely exposed parts of the beds. The entire exposed face of the beds is closely jointed and made up of a very loose jumble of concavo-convex spalls (each about 2 to 6 mm thick) representing the separated and fallen-off "peels" of expanded spher-

oidal exfoliar structures. The cores (kernels) of such clay structures are more rounded, harder, and contain higher silt and sand contents than their surrounding more clayey spalls. Some of the expanded onion-like peels do no readily fall away and the outcrop is made of closely packed spheroidal shells with diameters ranging between 4-8 cm.

Plate 1e. Spheroidal weathering of a marked bed in its outcrop at locality UB3. Inner rounded cores (kernels) are picked up from the spheroids. The inner zones of the structure are concentric with respect to the outer zones.

Mineralogically, these clay spheroids are made up mainly of montmorillonite with lesser amounts of quartz, illite and kaolinite; minor calcite and scarce chlorite. It is worthy to mention that the montmorillonite content was found to be higher in the spalls than in the cores of some spheroids (Table 1 and Figs. 2 & 3).

Ollier (1971) had reviewed the different hypotheses advanced to explain spheroidal weathering of different kinds of igneous and sedimentary rocks. Gindy *et al*. (1985) suggested that spheroidal weathering in marl and chalk is due to expansion of smectite and other expandable mixed-layer clays in concentric zones at the exposed free outer surface of the beds. The concentric structures were initiated by Liesegang diffusion of dew water into bed exposures, starting from spaces between joint and fracture polygons of the rock. Diffusion proceeded inwardly into the cores of the polygons producing alternating concentric zones of different tenacities.

Clay spheroids of Ubhur Formation are believed to be formed as a result of chemical weathering caused by diffusion of dew water through incipient joints and cracks present in the exposed silty to sandy clay beds. This leads to the ex-

TABLE 1. Identified clay minerals and their relative abundances in the clay fractions of the Ubhur Formation samples, based on X-ray diffraction analysis.

Locality no.	Sample no.	Montmorillonite (M)	Kaolinite (K)	Illite (I)	Chlorite (Ch)	Remarks
UB 1	1	+++++	+	++	–	Grayish white clay
	3	+++++	+	+	–	Contact between reddish & white clay
	4	+++++	+	++	+	Hard fissile sandy clay
UB 2	129	+++	+++	+++	–	Thin greenish grey clay band between massive gypsum & selenite
	130	++++	+++	++	–	Bottom of the quarry
UB 3	89A	++++	++	++	+	Core of spheroids
	90A	++++	++	++	+	Core of spheroids
	90B	++++	++	++	–	Spalls of spheroids
UB 4	91A	+++++	–	++	–	Core of spheroids
	91B	++++++	–	–	–	Spalls of spheroids

Symbols for approximate percentage contents are ++++++: > 90%; +++++: 70-90%; ++++: 50-70%; +++: 30-50%; ++: 10-30%; +: <10%; and –: not recorded.

pansion of montmorillonite which swells by simply absorbing water and subsequently will produce mechanical stresses by uneven volume changes in the surface as minerals decay. This will also cause the leaching of coarse ingredients as silty and sandy quartz and consequently increasing the montmorillonite content in the spalls of the spheroids.

Mineralogy of Clay and Evaporite Deposits

The mineralogy of the clay and evaporite deposits of Ubhur Formation have been investigated by X-ray diffraction using a PW 1840 Philips Diffractometer (Faculty of Earth Sciences, KAAU, Jeddah-KSA), and differential thermal and thermogravimetric analyses using the computerized Perkin-Elmer DTA 7 & TGA 7 units (National Research Center, Cairo, Egypt). Both tools gave similar results concerning the identification of clay and evaporite minerals.

A. Clay Deposits

1. X-ray Diffraction Analysis

Clay fractions of ten clayey samples representing the four studied localities were analyzed by X-ray diffraction. Four bulk samples were also analyzed to

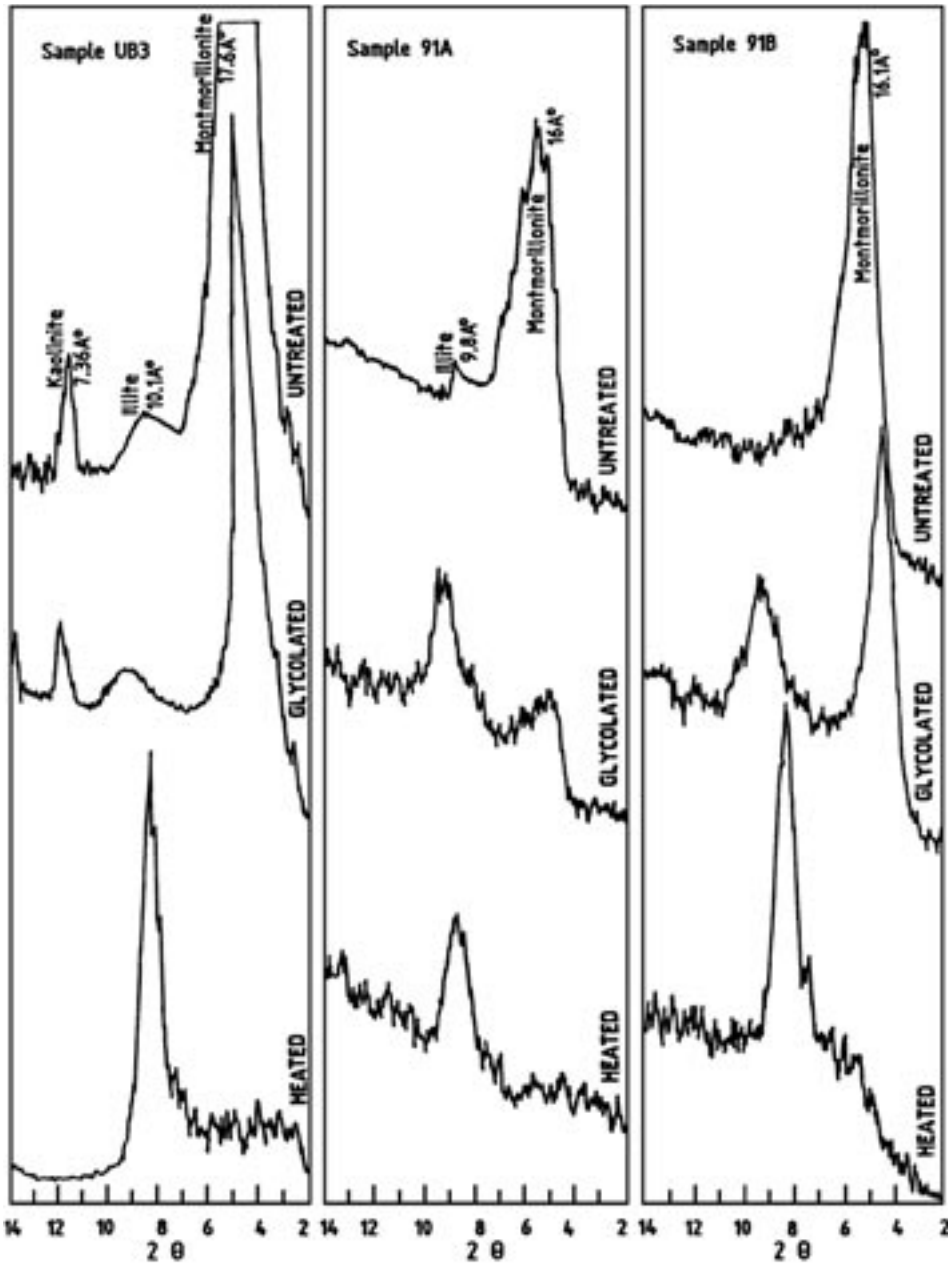

FIG. 2. X-ray diffraction patterns of the clay fraction (<2 μm) of three representative samples, Ubhur Formation.

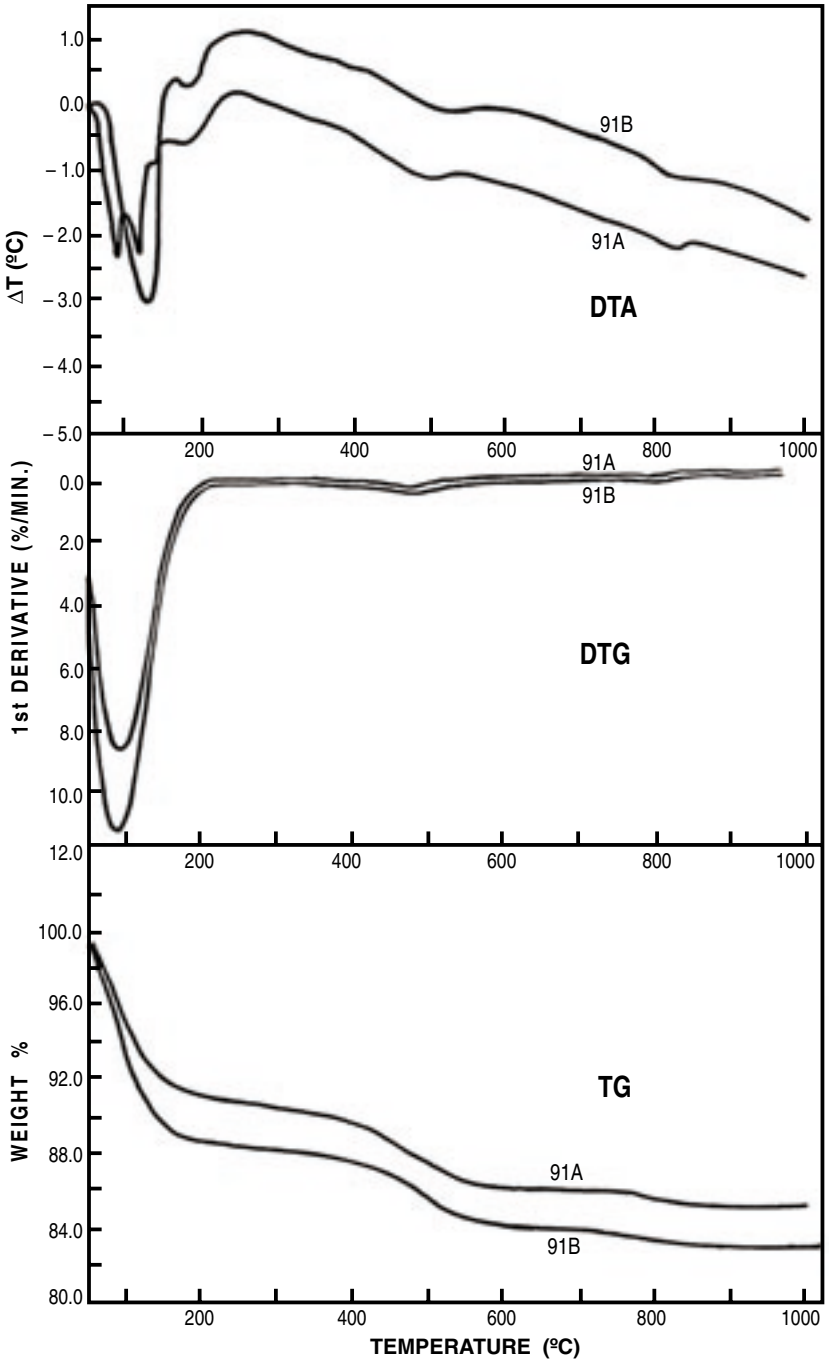

FIG. 3. Thermal curves of a spheroidal clay sample (clay fraction) from locally UB4 (91A represents the core and 91B represents the enveloping shells).

ascertain the associated non-clay minerals. The data of Brown and Brindley (1980) and Powder Diffraction File, JCPDS (1984) were used for minerals identification. The method of Pierce and Siegel (1969) was used for semiquantitative estimation of clay minerals content.

The results given in Table 1 show that montmorillonite (Ca^{++} and/or Mg^{++} rich variety) is the predominant mineral (Fig. 2) in the studied samples, ranging between 90 and 100% in 2 samples, between 70% and 90% in 3 samples and between 50 and 70% in 4 samples. Illite is recorded in 9 samples; in the range between 30-50% in one sample and between 10-30% in 7 samples and less than 10% in one sample. Kaolinite is recorded in 8 samples; ranging from 30-50% in 2 samples, 10-30 % in 3 samples and less than 10% in other 3 samples. Chlorite is rarely recorded, appearing in 3 samples with amounts less than 5%.

It is worth mentioning that montmorillonite content is higher in the spalls than in the core of some spheroids (Table 1 and Figs. 2 & 3). The least montmorillonite content is recorded in the clay deposits, which associate the evaporitic sequence of UB2.

X-ray diffractograms of the studied bulk samples indicate that quartz, k-feldspar and plagioclase feldspar are the main non-clay components.

2. Differential Thermal & Thermogravimetric Analyses

The results obtained by differential thermal and thermogravimetric analyses of the clay fractions mostly agreed with those of X-ray diffraction analysis and show that the samples are made up of montmorillonite with lesser amount of illite and kaolinite, and scarce chlorite. The results of two representative clay samples (representing a core (91A) and a spalls (91B) of a clay spheroid) are given in Table 2. Thermal curves for the samples are shown in Fig. 3. The DTA curve has a marked endothermic DTA peak below 200ºC. It is double in sample 91B and treble in sample 91A (Table 2 & Fig. 3) indicating that the montmorillonite present is of the Ca^{++} and / or Mg^{++} rich variety (Todor, 1976) and confirming that some mineralogical changes have been happened during clay spheroid formation. This DTA peak is mirrored by an endothermic DTG peak at about 90ºC and a substantial TG loss of mass, higher in sample 91B than in sample 91A (Table 2 and Fig. 3).

Higher temperature thermal effects are also endothermic and occur in two stages (510ºC-530ºC & 810ºC-830ºC), the first being more intense, and both are due to dehydroxylation, *i.e.*, the removal of OH group from clay mineral lattice.

A third minor thermal effect at about 850ºC, barely shown in Fig. 3, is exothermic. It immediately follows the dehydroxylation effects and is not accompa-

nied by any weight change. It is attributed either to structural reorganization or formation of high-temperature mineral phases such as mullite, cristobalite, etc. (Grim, 1968). An effect of this type is usually intense in kaolinite, minor in illite and is very minor in montmorillonite, which suggests the presence of minor illite in sample 91A (Table 2 & Fig. 3).

TABLE 2. Differential thermal and thermogravimetric analyses results of two representative clay samples and a selenite sample from Ubhur Formation.

Sample no.	Endoth. peak		Exoth. DTA peak	TG loss %	Description of DTA peak	Assignment of the reaction	Identified minerals
	DTA°C	DTG°C					
91A	89 120 165	90	–	9.2	mod., sharp Treble mod., sharp small	Removal of adsorbed water	Montmorillonite with some illite
	510 830	470 780	– –	5.2 0.7	Moderate, asym Small, broad	Dehyroxylation, *i.e.* removal of OH group	
			850	–	Very small, sym.	Structural reorganization	
91B	133 180	88	–	10.5	large, sharp Double small	Removal of adsorbed water	Totally montmorillonite
	530 810	478 790	– –	4.7 1.1	Moderate, broad Small to mod., asym.	Dehydroxylation, *i.e.,* removal of OH group	
	–	–	847	–	Very small, sym.	Structural reorganization	
88A	165 185	132	–	21.2	large, sharp Double large, sharp	Removal of water of crystallization	Pure gypsum
	–	–	368		Small, sym., broad.	Polymorphous transformation	

B. Evaporite Deposits

1. X-ray Diffraction Analysis

X-ray diffraction analyses were done on two evaporite samples from locality UB2, the results indicating that they consist entirely of gypsum. As shown by their diffractograms (Fig. 4), one has a higher degree of crystallinity (selenite sample 88A) than the other (gypsum sample 88B), which is massive and finely crystalline.

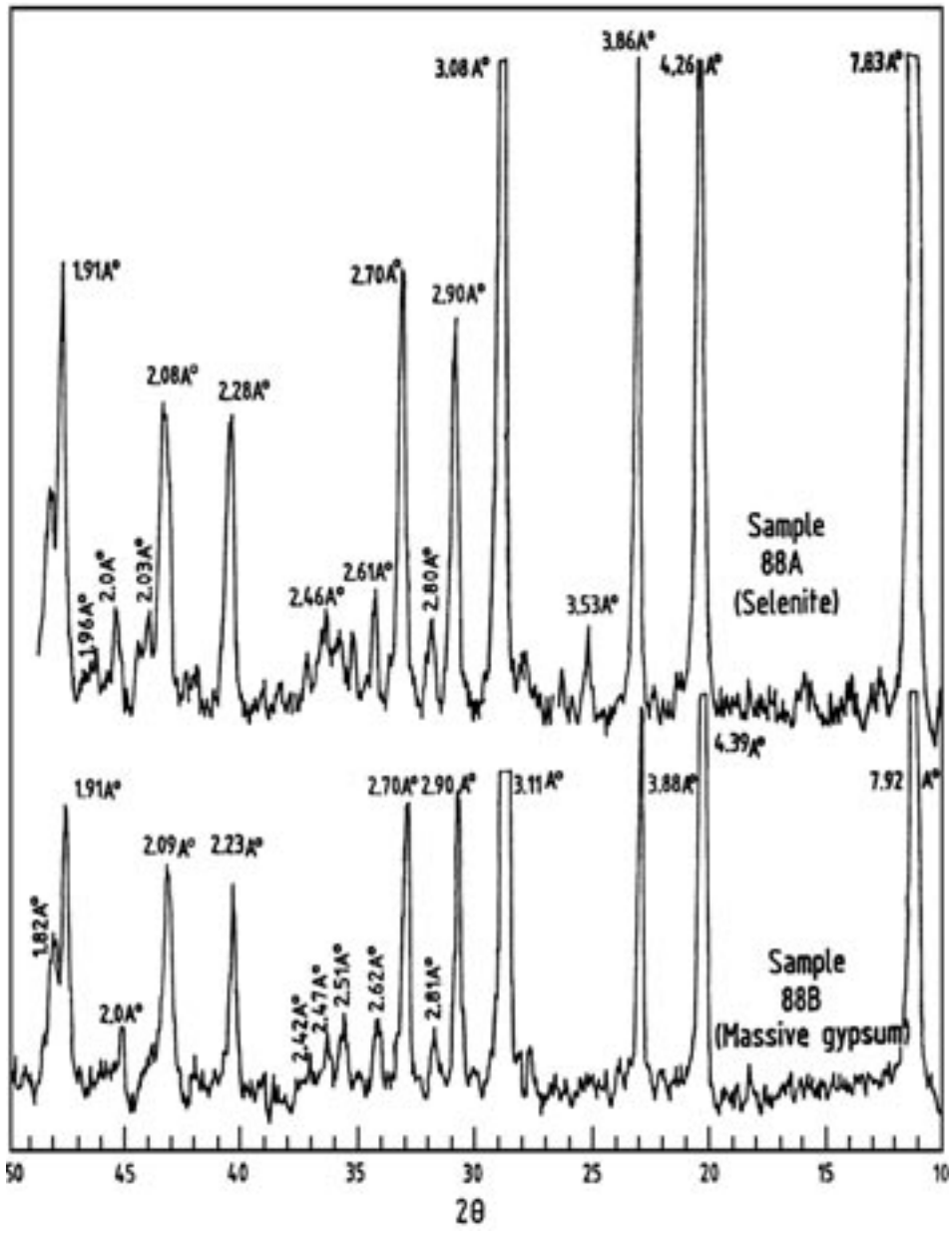

FIG. 4. X-ray diffraction patterns of the two evaporite samples of locality UB2.

2. Differential Thermal & Thermo Gravimetric Analyses

Differential thermal & thermogravimetric analyses results of the selenite sample are given in Table 2 and illustrated in Fig. 5. Thermal curves show two effects reflecting the removal of the water of crystallization. They are represented by two DTA peaks or "double DTA peak", the first at 165ºC due to the removal of 1½ water molecules (Todor, 1976) as a result of which gypsum passes into plaster. The other peak at 180ºC is due to the removal of the remaining half water molecule. For different prepared selenite concentrations, these peaks range from 142ºC to 163ºC and from 153ºC to 185ºC. Generally the peak temperature increases with concentration. It is worthy to mention that these two peaks, according to Liptay (1971) and Todor (1976), occur at 180ºC & 200ºC (In static air). The lower peak temperatures recorded in the present work may be due to the use of nitrogen atmosphere and to the small weights of samples used in all runs.

The two DTA peaks (or the double DTA peak) are associated with one DTG peak at 133ºC (112ºC to 132ºC for the different concentrations) and a TG loss of 21.2 % of the original sample weight (Table 2 & Fig. 5).

TG & DTG runs were also carried out for the investigated selenite sample using a Mettler TA 3000 apparatus (Umm Al-Qura University, Makkah-KSA). The curves obtained showed double endothermic DTG peak at 148ºC and 175ºC accompanied with TG loss of 21.2% of the original sample weight (Fig. 5).

Gypsum derivatograms reported by Liptay (1971) and Todor (1976) using a Hungarian-MOM apparatus show double DTG peak, similar to the double DTA peak in Fig. 5 and a minor deflection in the TG curve. By means of such double DTG peak and the TG curve deflection, it is possible to estimate precisely the TG loss percentage that corresponds to each peak. Such TG curve deflection also did not appear on curves of both the used Perkin-Elmer and Mettler apparatus.

After removal of water of crystallization, and on further heating, a new thermal transformation occurs, which is recorded only on the DTA curve as an exothermic peak at 369ºC (Fig. 5), and 361ºC to 367ºC for the other concentrations as a result of the polymorphous transformation of gypsum (Todor, 1976).

During the course of this work, nine concentrations (10%, 20%, etc. ... 90%) of the studied selenite sample were prepared by dilution and thorough mixing and homogenizing with α-alumina and subjected to thermogravimetric analysis. A linear relation was obtained between concentration and TG loss% (Fig. 6), and this relation can be used to estimate precisely the gypsum percentage in any unknown sample.

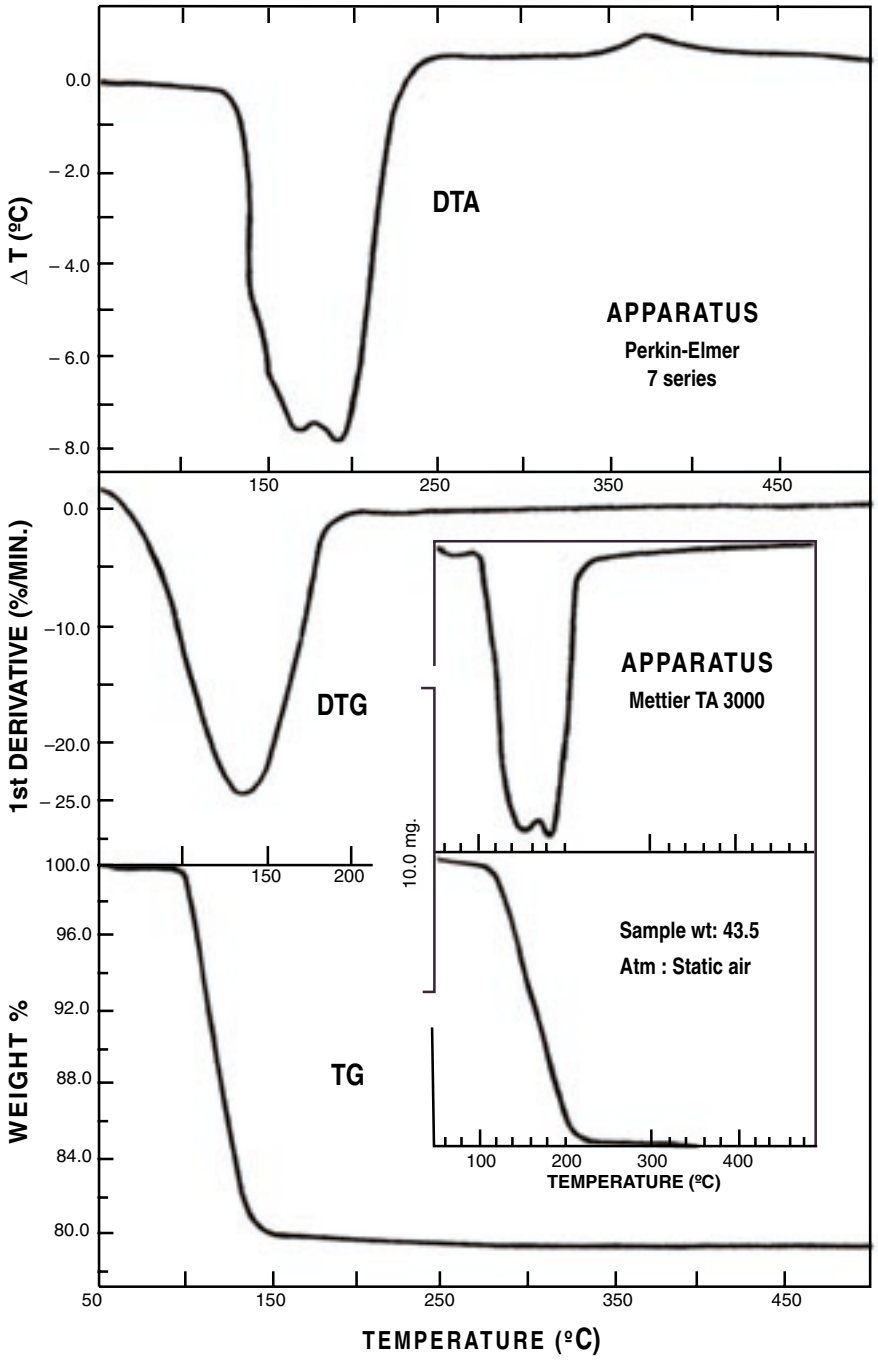

FIG. 5. Thermal curves of the gypsum (selenite) sample (88A), locality UB2.

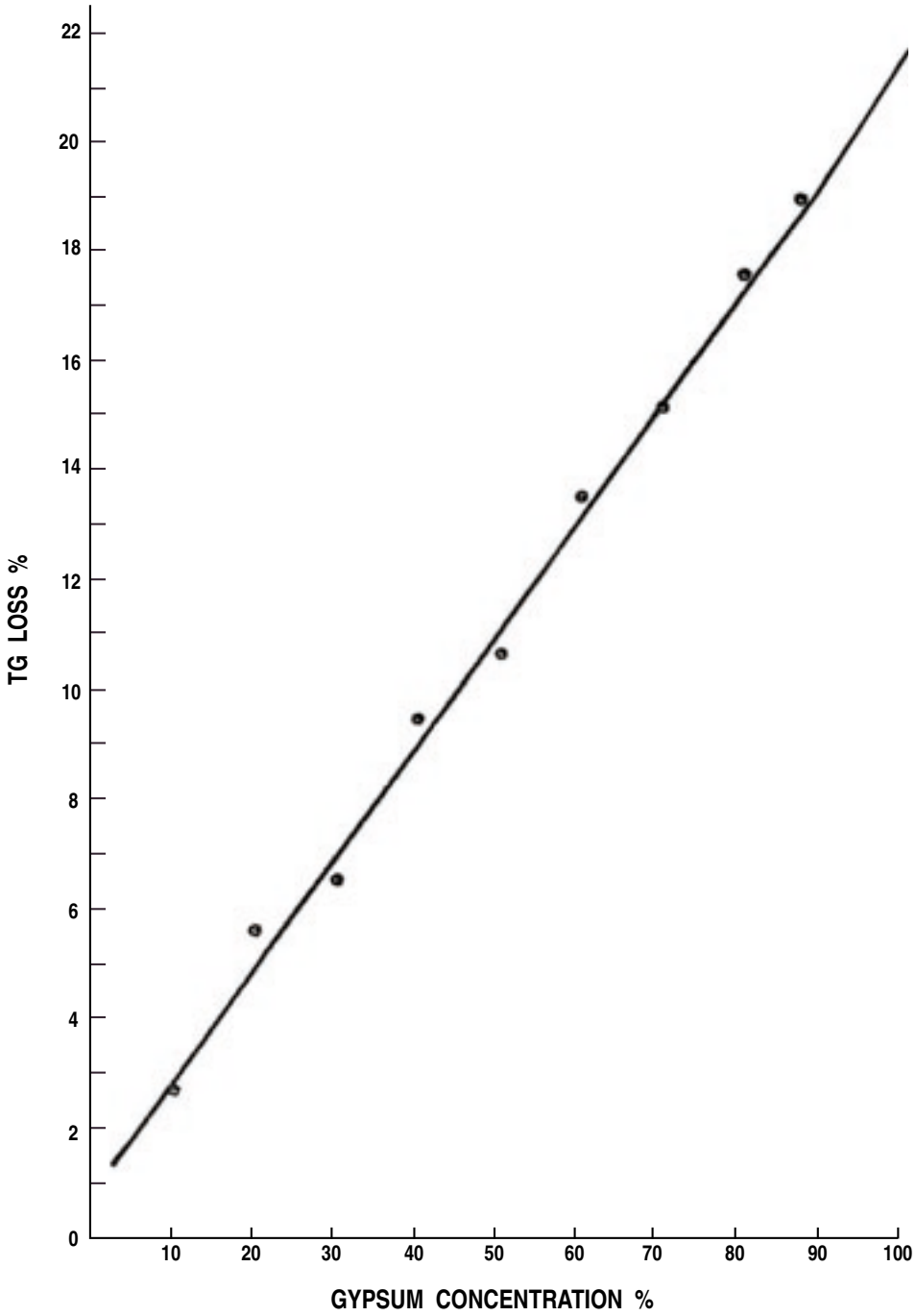

FIG. 6. Gypsum concentration versus TG loss % relation.

References

Andreieff, P. (1983) *Etude micropaleontologique de deux larves-minces, Arabie Saoudite.* Bureau de Recherches Geologiques et Minieres, Internal Report 83-GEO EM-55, 1 p.

Basyoni, M.H., El-Askary, M. A., Saad, N.A. and **Taj, R.J.** (2002) Mineralogy of the Tertiary clay deposits in Makkah and Rabigh quadrangles, west-central Arabian Shield, Saudi Arabia. *Jour. Sci. Res., Sultan Qaboos Univ., Oman* (in press).

Brown, G.F., Jackson, R.O., Bogue, R.G. and **Maclean, W.H.** (1963) *Geology of the Southern Hijaz quadrangle, Kingdom of Saudi Arabia*. Saudi Arabian Directorate General of Mineral Resources, Miscellaneous Geologic Investigations Map I-210A, 1:500,000 scale.

Brown, G. and **Brindley, G.W.** (1980) X-ray diffraction procedures for clay mineral identification. In: *Crystal structures of clay minerals and their X-ray identification* (Brindley, G.W. and Brown, G.ed.), Mineralog. Soc., London, 305-360.

Gindy, A.R., Al Shakiry, A.J. and **Saad, N.A.** (1985) Spheroidal weathering in marls and chalk of Gebel Gurnah near Luxor, Southern Egypt. *Jour. Sed. Petrol.*, **55:** 762-768.

Grim, R.E. (1968) *Applied clay mineralogy.* McGraw-Hill Book Company Inc., New York, Toronto, London, 422 p.

Liptay, G. (1971) *Atlas of thermoanalytical curves*. Akademiai Kiado, Budapest, Heyden & Son Ltd., London, 116 p.

Moore, T.A. and **Al-Rehaili, M.H.** (1989) *Explanatory notes to the geologic map of the Makkah Quadrangle,* sheet 21D, Kingdom of Saudi Arabia. DGMR, Jiddah, Saudi Arabia.

Ollier, C.D. (1971) Causes of spheroidal weathering. *Earth Sci., Reviews.* V. **7,** 127-141.

Pierce, J.W. and **Siegel, F.R.** (1969) Quantification in clay mineral studies of sediments and sedimentary rocks. *Jour. Sed. Petrol.*, **39**: 187-193.

Powder Diffraction File (1984) *Inorganic phases*, JCPDS. Inter. Center for diffraction data, Pennsylvania, USA.

Rouchy, J.M. (1980) *The evaporitic sequences of the terminal Miocene of Sicily and of Southern Spain*. Evaporite Deposits, Editions Technip, Paris, 34-39.

Shearman, D.J. (1980) Sebkah facies deposits. In: *Evaporite Deposits, illustration and interpretation of some environmental sequence*, Edition Technip, Paris.

Spencer, C.H. and **Vincent, P.L.** (1984) *Bentonite resources potential and geology of Cenozoic sediments, Jeddah region.* Saudi Arabian Deputy Ministry for Mineral Resources Open-File Report BRGM-OF-04-31, 60 p.

Taj, R.J., El Askary, M.A., Saad, N.A. and **Basyoni, M.H.** (2001a) Sedimentology, mineralogy, chemistry and industrial applications of argillaceous rocks in some localities in Makkah and Rabigh quadrangles, west-central Arabian Shield, Saudi Arabia. *Sponsored research study by King Abdulaziz University,* Project No. 203/419 (final report).

Taj, R.J., El Askary, M.A., Saad, N.A. and **Basyoni, M.H.** (2001b) Eonomic potentiality of the Tertiary clay deposits in Makkah and Rabigh quadrangles, west-central Arabian Shield, Saudi Arabia. *5th Int. Conf. on Geochemistry, Alex. Univ., Egypt*, Vol. **2,** 169-183.

Taj, R.J., Saad, N.A., El Askary, M.A. and **Basyoni, M.H.** (2002) Geochemistry and origin of the Tertiary clay deposits in Makkah and Rabigh quadrangles, west-central Arabian Shield, Saudi Arabia (in preparation).

Todor, D.N. (1976) *Thermal analysis of minerals.* Abacus Press, Tunbridge Wells, Kent, 256 p.

دراسة معدنية مع بعض الظواهر الرسوبية لمتكون أبحر شمال جدة ، المملكة العربية السعودية

ر. ج. تاج* ، م. أ. العسكري، ن. أ. سعد**، م. ح. بسيوني***

**كلية علوم الأرض ، جامعة الملك عبد العزيز ، جـدة – المملكة العربية السعودية*

***قسم الجيولوجيا ، كلية العلوم ، جامعة الإسكندرية*

الإسكندرية – جمهورية مصر العربية

المستخلص. يختص البحث بدراسة المحتوى الطيني والمتبخرات لمتكون أبحر ، حيث تم دراسة التركيب المعدني بواسطة أجهزة قياس حيود الأشعة السينية ، والتحليل الحراري التفاضلي والوزني . ويسود معدن المونتموريلونيت (النوع الغني بالكالسيوم أو الماغنسيوم) بالرواسب الطينية ، ويليه تواجداً معدن الأليت ثم الكاولينيت ، وكذلك سجل وبكميات ضئيلة معدن الكلوريت . وقد أظهر السطح المكشوف من هذه الرواسب درجات مختلفة من التجوية الكروية . والتكور الناتج ما هو إلا نتيجة لتمدد معدن المونتموريلونيت وذلك عن طريق امتصاص الماء المصاحب لغسل بعض المكونات الخشنة وبعض التغيرات المعدنية لهذه الرواسب. وتتمثل رواسب المتبخرات بنوعان من الجبس أحدهما مصمت دقيق التبلور بينما الآخر من السيلينيت الصافي. وفي الجزء العلوي المكشوف من السيلينيت تتشكل ورود الصحراء الناتجة عن عمليات مابعد الترسيب (التحور). وقد أشير إلى أنها تكونت بفعل المياه الجوفية المتخللة والمحملة بكبريتات الكالسيوم المذابة والمشبعة لسطح الراسب مرسبة الجبس كورود الصحراء في الفترات الشديدة الجفاف. وقد أظهرت نتائج التحليل الحراري الوزني لعينات سلينيت عديدة مختلفة التركيز تم تجهيزها، علاقة خطية واضحة بين التركيز والنسبة المئوية لمقدار الفاقد المائي، ومن الممكن استخدام هذه العلاقة في التقدير الدقيق للنسبة المئوية للجبس لعينات مجهولة.